

The Surface Albedo of the Earth in the Near Ultraviolet (330-340 nm)

J E FREDERICK

NASA/Goddard Space Flight Center, Laboratory for Planetary Atmospheres, Greenbelt, Maryland 20771

and

R B ABRAMS

Computer Sciences Corporation, Silver Spring, Maryland 20910

Satellite-borne measurements of solar radiation backscattered by the earth and atmosphere allow a determination of the surface albedo in the near ultraviolet. Combination of the data obtained by the backscatter ultraviolet instrument on the Atmosphere Explorer-E satellite with a numerical model of radiative transfer including multiple scattering and surface reflection has yielded albedos at tropical latitudes during a 15-month period in 1979-1980. The wavelengths studied are 331.2 and 339.8 nm. Sixty-nine percent of the measurements imply albedos less than 0.3. Higher values include a contribution due to reflection from clouds and are consistent with previous estimates of the fractional cloudcover in the tropics. An albedo histogram based on a bin width of 0.1 shows results in the range 0.1-0.2 to be the most frequent, appearing in 29% of the cases, although values which span the entire range 0.0-1.0 are present. The derived albedos show no correlation with solar zenith angle. This result is consistent with the fact that, at the wavelengths considered, the diffuse integrated intensity is larger than the attenuated direct solar beam near the ground.

Introduction

Reflection of incoming solar energy by the earth's surface and by clouds has a significant impact on global climate and biological systems (SMIC, 1971). For purposes of climate modeling, the relevant parameter is the albedo integrated over all wavelengths, the major contribution coming from the visible portion of the spectrum. Considerable information concerning the albedo of various surfaces and of the planet as a whole is now available for the visible region (Kondratyev, 1973, Hummel and Reck, 1979). Such is not the case in the near ultraviolet, although a limited amount of information does exist (Kondratyev, 1973, Doda and Green, 1980). At wavelengths below 290 nm the

solar irradiance is effectively screened from the earth's surface by strong absorption due to ozone. However, wavelengths extending up to 340-350 nm are relevant in biological and photochemical applications. An impetus for study of the stratosphere concerns the role of ozone as a shield against the ultraviolet solar irradiance which is harmful to living organisms. In this context, the fractional cloudcover and the cloud albedo are important parameters since clouds act as a shield for the earth's surface. In photochemical studies, models of the troposphere and lower stratosphere require inclusion of multiple scattering and surface reflection for the calculation of dissociation rates (Luther and Gelinas, 1975, Matloff and Stewart, 1980). For example, the produc-

tion of $O(^1D)$ in the dissociation of ozone occurs in the wavelength region 290–320 nm at tropospheric altitudes. Reactions of these excited oxygen atoms with N_2O and H_2O then provide the major sources for nitric oxide and hydroxyl radicals which remove ozone catalytically. Although the radiation reflected by a low-albedo surface such as the ocean has a minor effect on the ozone dissociation rate, over a highly reflecting cloud deck the destruction will be significantly enhanced. These considerations illustrate the importance of obtaining information on the earth's surface albedo in the near ultraviolet.

Orbiting platforms provide an effective means of obtaining albedo information over a large geographic region. In this study, we derive surface albedos from the data base collected by the backscatter ultraviolet (BUV) monochromator on the Atmosphere Explorer-E (AE-E) satellite from an orbit inclined at 20° to the equator. The period of operation considered here is January 1979 through March 1980. The analysis utilizes radiances which emerge from the atmosphere in the vertical at wavelengths 331.2 and 339.8 nm which are outside the region of strong absorption by ozone. However, since albedo varies slowly with wavelength (Kondratyev, 1973) the results should be representative of the entire near ultraviolet region. A radiative transfer model which includes all orders of multiple scattering allows elimination of the signal due to molecular backscatter. The reported albedos therefore represent properties of the lower boundary of the atmosphere (clouds, ocean, soil, vegetation) subject to limitations of the numerical model which we discuss in detail. The goal of this work is to determine the frequency of occurrence of various al-

bedos in the tropics for future use in studies of the diffuse radiation field and trace gas photodissociation rates in the troposphere and lower stratosphere. This emphasis differs from previous work such as that by Doda and Green (1980) who measured the reflectances of selected surfaces. Our focus is on determining the range of albedos encountered in observations over a large geographic region as opposed to associating a given albedo value with a specific type of terrain.

The Experiment and Radiative Transfer Treatment

The BUV experiment on AE-E is identical to that on the Nimbus 4 satellite which has been described by Heath et al. (1973). The instrument observes the backscattered solar ultraviolet radiance which exits the atmosphere in the vertical at 12 wavelengths with a spectral resolution of 1 nm. Data at wavelengths less than 300 nm provide information on the vertical distribution of ozone in the upper stratosphere (Frederick et al., 1978, 1980). For the albedo analysis we restrict attention to the two longest wavelength signals, 331.2 and 339.8 nm, which are attenuated only slightly by ozone but are significantly influenced by reflection at the lower base of the atmosphere. For the time period 1979–1980, considered in this paper, the satellite was in a circular orbit at an altitude of 460 km and the 11° instrument field of view projected onto the earth's surface as a square approximately 88 km on a side. Figure 1 presents the data obtained at 339.8 nm along a typical orbit plotted against solar zenith angle which is the relevant independent variable in the radiative transfer theory. The maxima in the measured radiances

indicate the passage of clouds through the field of view while smaller variations are related to the underlying terrain For comparison, the solid line in Fig 1 is a theoretical calculation which assumes a surface albedo of zero

The quantity required for the deduction of lower boundary albedos is the ratio of the emergent backscattered radiance, I , to the incident solar irradiance, F , both of which are available from the BUV instrument. However the derived absolute value of this ratio depends on the optical properties of a diffuser plate used during direct solar observations but not for the backscattered radiance measurements. As discussed by Frederick et al (1980), the I/F values obtained from

the instrument appear to have a systematic error and we have therefore introduced calibration factors at 331.2 and 339.8 nm to place the backscatter ratios on a reliable absolute scale. To derive these corrections we compared all measured radiances for 1979–1980 with calculations based on a surface albedo of zero. The ratio of measured to computed radiance can never be less than unity if the instrument is properly calibrated This procedure indicated that no systematic instrument degradation had occurred over the operating period, however, a time-independent adjustment was required in the absolute radiances These calibration factors were derived by first taking ratios of measured to computed radiances for

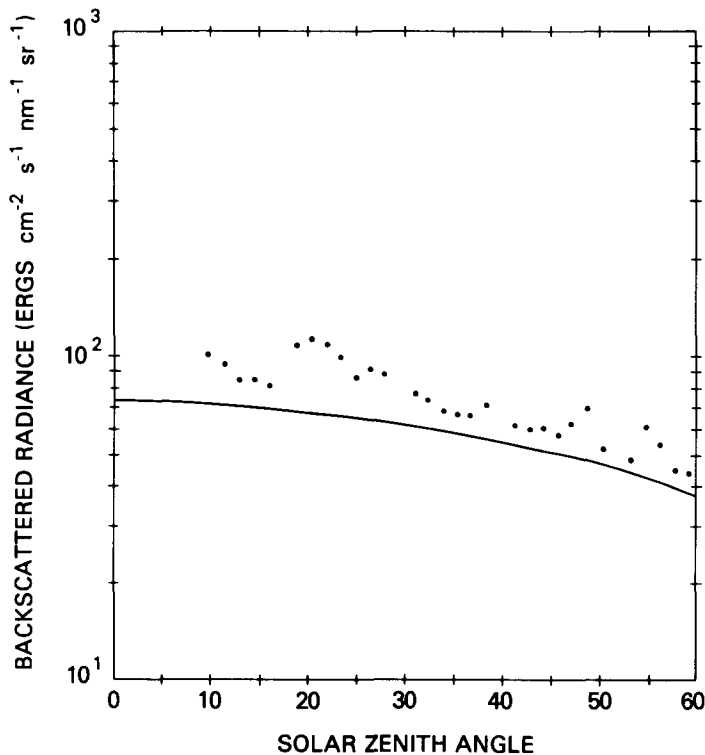


FIGURE 1 Backscattered radiances at 339.8 nm measured during a typical orbit of AE-E (dots) Solid line represents a theoretical calculation for clear-sky conditions and a surface albedo of zero

the entire 1979–1980 data base. All ratios less than one which fell within 5% of the lowest value in the data set were averaged and their standard deviation taken. The correction for each wavelength is then defined to be the multiplicative factor which makes this average ratio equal to unity. Table 1 presents the corrections that we estimate to be as accurate to $\pm 2\%$ based on the standard deviations. The values so derived are consistent with those inferred by Frederick et al. (1980) for shorter BUV wavelengths by comparison of measured radiances with values computed from a standard tropical ozone profile obtained by rocket measurements.

For the albedo determination, we use a numerical model of radiative transfer which assumes a plane parallel atmosphere, includes all orders of multiple scattering, absorption by ozone, and reflection at a Lambertian lower boundary whose albedo and altitude are specified. The numerical technique has been described in detail by Herman and Browning (1964). At the wavelengths considered the optical depth due to ozone absorption is small, and in the tropics ozone varies little in time, so it suffices to adopt a single model for all calculations. The average of the ozone profiles reported by Krueger (1973) measured within 22° of the equator is a suitable choice.

Figure 2 shows the variation of the computed I/F ratios at 339.8 nm for various albedos and altitudes of the lower

surface. As expected, for a fixed lower boundary altitude, the backscattered radiance increases with surface albedo. However, the variation of the signal with the altitude of the lower boundary differs in sign according to the surface albedo. For an albedo of $A=0.2$ the signal increases as the altitude of the reflecting surface rises while the opposite behavior exists for $A=0.6$. Near $A=0.4$ the emergent radiance is nearly independent of the height of the lower boundary. These effects are better illustrated in Fig. 3 for a fixed solar zenith angle of 40° and lower boundaries at $Z_b=0, 8$, and 16 km. This behavior may be understood by considering the following limiting cases. For an albedo of zero, the radiance which emerges from an atmosphere with a lower boundary at 0 km must be larger than that with the boundary placed at 16 km due to the contribution from Rayleigh scattering in the lowest 16 km. However, if a surface with an albedo of unity were placed at 0 km one gets less emergent radiance than for the same albedo at 16 km. This arises from the fact that Rayleigh scattering depletes the upward reflected beam causing a radiation trapping effect in the lower atmosphere. Absorption by ozone below 16 km acts in the same sense but has a negligible effect. If there were no depletion of the upward beam after reflection at the ground, then the upward radiation at 16 km, which consists of both a Rayleigh backscattered component and

TABLE 1 Calibration Factors Applied to BUV Radiances to Place Them on a Reliable Absolute Scale

WAVELENGTH (nm)	DERIVED CALIBRATION FACTOR	POSSIBLE RANGE OF CALIBRATION FACTOR
331.2	1.149	1.126–1.172
339.8	1.116	1.094–1.138

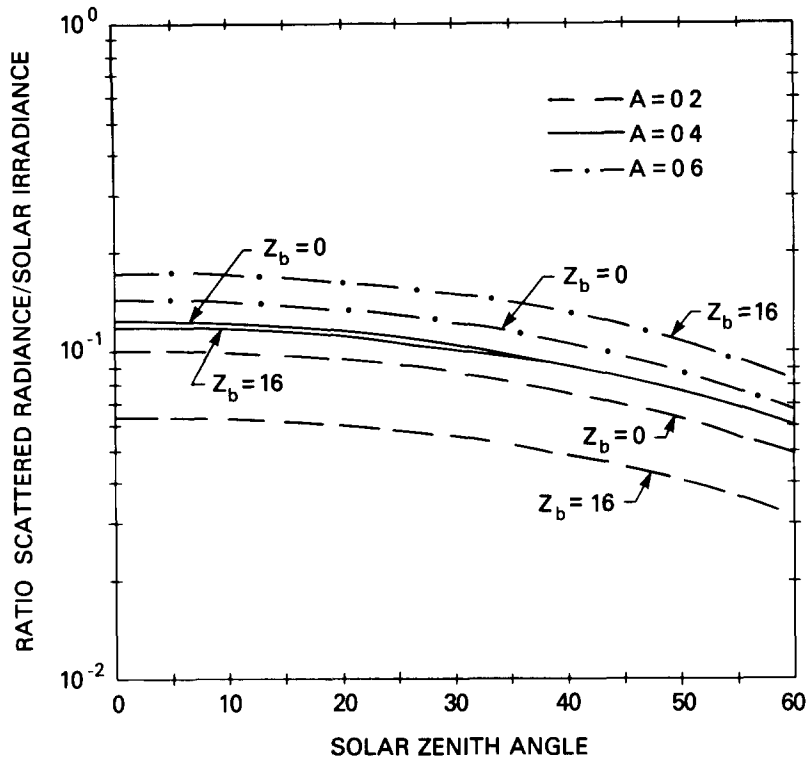


FIGURE 2 Computed ratios of backscattered radiance to solar irradiance at 339.8 nm for albedos of $A = 0.2, 0.4$, and 0.6 and altitudes of the base of the atmosphere at $Z_b = 0$ and 16 km

the ground component, would equal that due to reflection off surface with $A=1$ placed at 16 km

Albedo
Determination and Error Sources

We deduce surface albedos by comparing the measured I/F at 331.2 and 339.8 nm with a grid of values computed for a range of albedo and solar zenith angles. Linear interpolation between computed I/F results defines an albedo that reproduces the measurement. To avoid inaccuracy due to the assumption of a plane parallel atmosphere, we use only data obtained at solar zenith angles less than 60° . We then derive initial albedos, denoted by A_0 , assuming the reflecting base of the

atmosphere to lie at $Z_b = 0$ km. This is clearly incorrect for larger albedos which represent scattering from clouds. Albedos less than 0.3 indicate reflection primarily at the ground ($Z_b = 0$) so the final albedo, A , is taken as equal to A_0 . Values in the range $A_0 = 0.3-0.4$ are essentially independent of the assumed reflecting height as shown by Fig. 3, so again we adopt $A \approx A_0$. For $A > 0.4$ reflection from cloud tops is surely involved and it is necessary to make a subjective choice as to the altitude of the base of the atmosphere. At tropical latitudes, cumulonimbus tops frequently reach 8 km in altitude and can occasionally build up tropopause heights near 16 km (Riehl, 1954). An average cloud-top height for the tropics is likely somewhat higher than

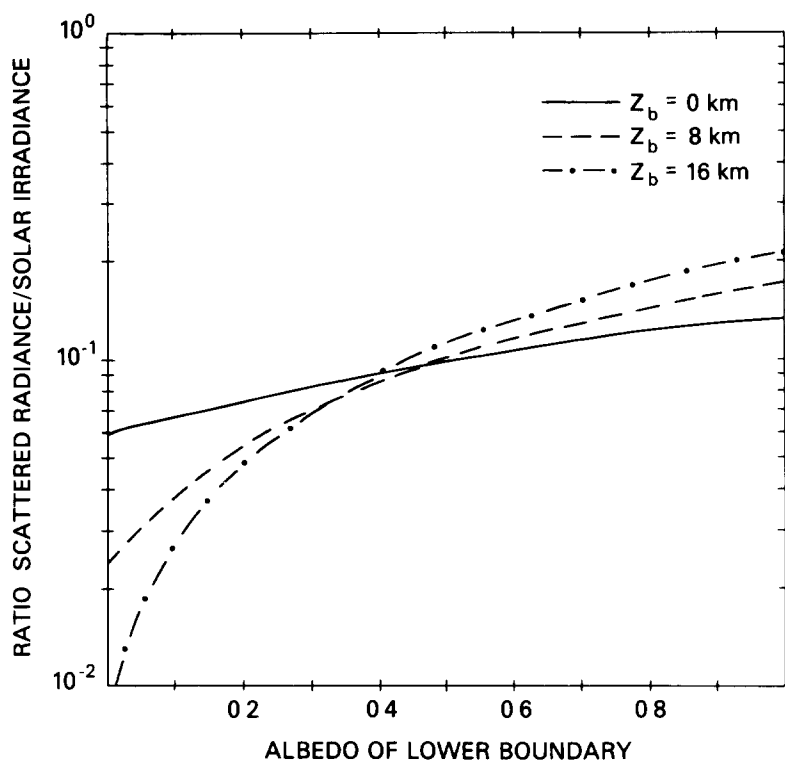


FIGURE 3 Computed variations of backscattered radiance/solar irradiance ratio with albedo of lower boundary. Altitude of the lower boundary is assumed to be at 0, 8, and 16 km and the wavelength is 339.8 nm.

the global average of 5.5 km (SMIC, 1971) and we choose to evaluate final albedos at $Z_b = 6$ km whenever $A_0 > 0.4$. Figure 4 illustrates the dependence of deduced albedo on the assumed lower boundary altitude for three particular I/F measurements at 339.8 nm and allows one to assess the likely error involved in the rather arbitrary choice $Z_b = 6$ km. If we adopt albedos deduced for the range $Z_b = 4$ –8 km as encompassing the likely uncertainty, then a reported value of $A = 0.55$ for $Z_b = 6$ km represents a possible range of $A = 0.53$ –0.57, an insignificant spread. Similarly the result $A = 0.79$ for $Z_b = 6$ km corresponds to the range $A = 0.76$ –0.88, which is at worst an error of 11.4%. We therefore conclude that the

need to specify the lower boundary altitude does not introduce severe errors into the albedo determination. Note in Fig. 4 that results $A_0 > 1.0$ are possible. These merely indicate that a high-altitude cloud deck with large albedo returns more scattered sunlight to space than is physically possible with a surface at $Z_b = 0$. Placement of the reflecting surface at higher altitude removes this inconsistency.

Several caveats must be associated with the albedo determination described above.

First, the radiative transfer model assumes the lower surface to be a Lambertian reflector giving an isotropic upward intensity regardless of the angular distribution of the incident radiation. Since

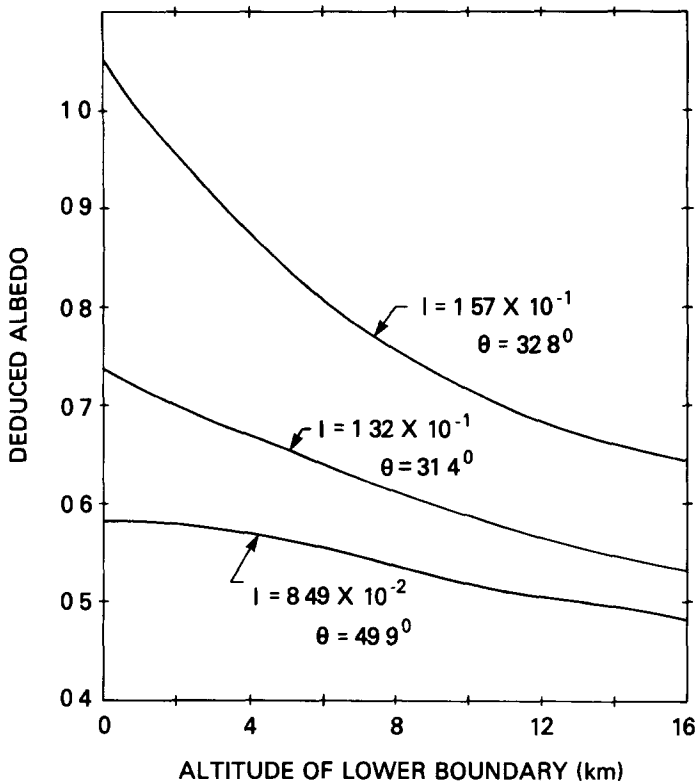


FIGURE 4 Dependence of deduced albedo on altitude of the lower boundary. Each curve corresponds to a single measured radiance, I , and solar zenith angle, θ .

land areas (soil, vegetation) are reasonably close to Lambertian (Hummel and Reck, 1979) this simplification is not serious here. However, clouds and water surfaces are highly non-Lambertian. Nonetheless, in the near ultraviolet the Lambertian assumption is still acceptable since the downward radiation field has a diffuse component at low altitudes comparable to or larger than the attenuated direct beam. So long as the reflection process uniquely maps the downward radiation in a specific direction into an upward beam in another well-defined direction, the surface is adequately described by the Lambertian approximation. This would be a poor assumption in

the visible region of the spectrum where the diffuse flux near the ground is small compared to the direct solar beam. However, the larger Rayleigh scattering cross sections in the near ultraviolet make the atmosphere act as an effective diffuser. Even reflection of the direct solar beam from clouds or an ocean surface, containing a complex spectrum of surface waves, will lead to a range of angles in the upward radiation field due to the irregular nature of these surfaces. Hence, although one cannot rigorously justify the assumption of a Lambertian surface, there is no other obvious model that could be applied with greater confidence. The final problem concerns the fact that the re-

flecting surface is not necessarily uniform over the BUV field of view. When the altitude of the lower atmospheric boundary is constant over the 88-km² field of view, the derived albedo is simply the horizontally averaged value. The interpretation is complicated when the area includes both clouds and ground. There is no general way to treat such cases without knowing the fraction of the field of view covered by clouds. The albedo derived in these circumstances will accurately reproduce the emergent radiance but does not represent the physical properties of a particular type of surface.

Results

Useful data were available during 267 orbits in the time period January 1979 through March 1980 giving a total of 7421 radiance measurements at each of the wavelengths 331.2 and 339.8 nm. The reported albedos are averages of the results derived for these two wavelengths. Differences between values deduced at 331.2 nm and those for 339.8 nm were typically 10–11% of the mean result. Although the true albedo is somewhat dependent on wavelength (Kondratyev, 1973), systematic error in the derived values due to uncertainty in the instrument calibration is surely larger than any true spectral dependence over the short span between the two wavelength measurements.

Figure 5 presents a histogram of the derived albedos sorted into bins of width 0.1. Error bars placed at the bin centers indicate the spread associated with the extreme instrument calibration factors given in Table 1. Use of the lower limit factors yields consistently smaller albedos and produces values denoted by the up-

per portion of the error bars in the bins $A=0.0-0.1$ and $A=0.1-0.2$ of Fig. 5. This limit also yields the lower end of the error bars in all of the bins with albedo greater than 0.2. Although the error bar on the percent occurrence of $A=0.0-0.1$ is rather large, being 35–40% of the best estimate, the qualitative pattern shown by the histogram is not altered by consideration of the maximum likely error. Albedos less than 0.3 appear in 61.3% of the measurements with values in the range 0.1–0.2 being the most frequent, occurring in 28.6% of the cases. A typical average cloud albedo lies in the range 0.5–0.6 where the AE data show a small secondary maximum. Albedos greater than 0.3 surely contain a contribution from clouds and account for 38.7% of the measurements with 27.7% of the total lying above $A=0.4$ where reflection from clouds provides the dominant contribution. These results are consistent with recent estimates of an approximate 30% cloudcover within 20° latitude of the equator (Curran et al., 1978).

Two features in Fig. 5 deserve special attention. First a large spread in cloud albedo appears in the tropics with values greater than 0.8 appearing in 4.4% of the cases. The wide range of albedos encompassed by clear and cloudy skies implies substantial variability in the diffuse radiation field available for dissociation of ozone and nitrogen dioxide. In view of this, study of possible horizontal variations in trace gases forced by a variable diffuse flux is of interest. Secondly, at the latitudes observed by the AE-BUV instrument, the ratio of water to land area is roughly 3 to 1. Hence, at least some albedos in the bin $A=0.2-0.3$ result from observations over oceans. Kondratyev (1973) has tabulated albedos for reflection

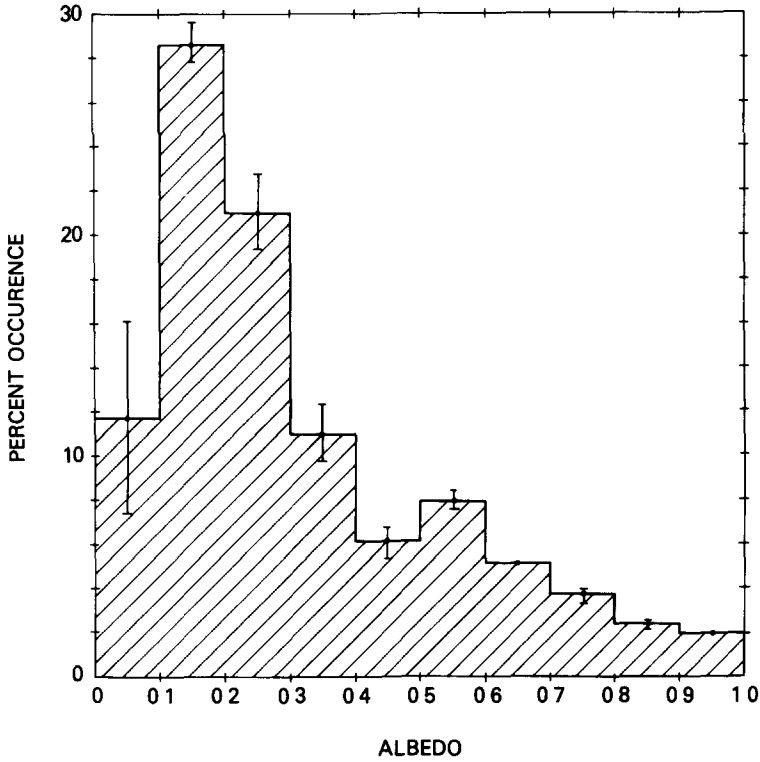


FIGURE 5 Histogram giving percent occurrence of albedos in bins of width 0.1. Figure covers the time period January 1979 to March 1980 and includes 7421 measurements at each of the wavelengths 331.2 and 339.8 nm.

of a direct beam from a flat water surface at a wavelength of 303 nm as computed from Fresnel's equation. The values range from $A=0.023$ for an overhead sun to 0.064 and 0.356 for solar zenith angles of 60 and 75°, respectively. A direct comparison between results of such a simplified calculation and true reflection from the ocean is not valid due to the presence of surface waves and particularly because of the large diffuse component of the incident radiation. Nonetheless, the BUV-derived albedos appear rather large since the highest solar zenith angle used is 60°. The most obvious explanation for the high albedos is the presence of a small frac-

tional cloudcover in the field of view or reflection from particulates or water droplets near the ocean surface. The albedos of most surfaces for direct radiation depend on the angle of incidence (Hummel and Reck, 1979). This variation, of course, vanishes in the presence of a purely isotropic radiation field. To seek any systematic solar zenith angle dependence in the derived albedos we have computed the correlation coefficient, r , between albedo and solar zenith angle based on linear regression. For all albedos $A \leq 0.4$ we find $r = -0.0025$ and for $A \geq 0.5$, $r = 0.048$. These values indicate a total absence of correlation and we

may therefore neglect any surface albedo variation with solar zenith angle in the near ultraviolet. This behavior is consistent with results tabulated by Kondratyev (1973) for the visible region of the spectrum. In the presence of total sky radiation, direct plus diffuse, albedos show much less dependence on solar zenith angle than when direct radiation alone is present. In the ultraviolet, the diffuse component is sufficiently large that albedo variations are totally obscured. For an ocean surface, the angular variation is further reduced by the presence of surface waves which effectively provide a range of incident angles even for a direct beam.

Discussion

Albedos derived from the AE-BUV data base span the entire range $A=0.0$ to near 1.0 with values of $A=0.1-0.2$ being the most frequent. This wide spread causes a substantial variability in the diffuse radiation field both above and below cloud level since the varying albedo of clouds implies a corresponding range in transmission. Above the cloud tops the diffuse radiation field competes with the direct solar beam in photodissociation processes while below a cloud base only the transmitted radiation is available to drive tropospheric photochemistry. The albedo histogram of Fig 5 allows one to predict the percentage occurrence of various diffuse radiation intensities and photodissociation rates. Use of the derived albedos in photochemical calculations will allow one to define the mean state composition of the tropical atmosphere and, equally important, the range of natural variability induced by the changing reflecting properties of the lower boundary.

References

- Curran, R J, Wexler, R, and Nack, M L (1978), Albedo climatology analysis and the determination of fractional cloud cover, *NASA Technical Memorandum*, 79576, pp 37
- Doda, D D, and Green, A E S (1980), Surface reflectance measurements in the UV from an airborne platform, Part 1, *Appl Opt* 19 2140-2145
- Frederick, J E, Guenther, B W, Hays, P B, and Heath, D F (1978), Ozone profiles and chemical loss rates in the tropical stratosphere deduced from backscatter ultraviolet measurements, *J Geophys Res* 83 953-958
- Frederick, J E, Abrams, R B, Dasgupta, R, and Guenther, B (1980), Natural variability of tropical upper stratospheric ozone inferred from the Atmosphere Explorer backscatter ultraviolet experiment, *J Atmos Sci* 38 1092-1099
- Heath, D F, Mateer, C L, and Krueger, A J, (1973) The Nimbus-4 backscatter ultraviolet (BUV) atmosphere ozone experiment—Two years operation, *Pure Appl Geophys* 106-108 1238-1253
- Herman, B M, and Browning, S R (1965), A numerical solution to the equation of radiative transfer, *J Atmos Sci* 22 559-566
- Hummel, J R and Reck, R A (1979), A global surface albedo model, *J Appl Meteor* 18 239-253
- Kondratyev, K Y, (ed) (1973), *Radiation Characteristics of the Atmosphere and the Earth's Surface*, New Delhi, Amerind Pub Co, (translated from Russian), pp 192-247
- Krueger, A J, (1973) The mean ozone distribution from several series of rocket soundings to 52 km at latitudes from 58° to 64°N, *Pure Appl Geophys*, 106-108 1272-1280

- Luther, F M and Gelnas, R J (1976), Effect of molecular multiple scattering and surface albedo on atmospheric photodissociation rates, *J Geophys Res* 81 1125–1132
- Matloff, G L and Stewart, R W (1979), Tropospheric UV flux calculations and photolysis rates for use with zonally and diurnally averages models, *Appl Opt* 18 3421–3425
- Riehl, H , (1954) *Tropical Meteorology*, New York, McGraw-Hill Book Co , pp 131–134
- SMIC, (1971) *Report of the Study of Man's Impact on Climate, Inadvertent Climate Modification*, Cambridge, Mass , The MIT Press, pp 110–122

Received 21 October 1980